Materials Research Bulletin 119 (2019) 110541

Contents lists available at ScienceDirect

Materials Research Bulletin

journal homepage: www.elsevier.com/locate/matresbu

Influence of polymer insertion on the dielectric, piezoelectric and acoustic properties of 1-0-3 polyurethane/cement-based piezo composite

A.O. Sanches[a,*], G.F. Teixeira[b], M.A. Zaghete[c], E. Longo[d], J.A. Malmonge[a], M.J. Silva[e], W.K. Sakamoto[a]

[a] Universidade Estadual Paulista (UNESP), Faculdade de Engenharia, Câmpus de Ilha Solteira. Av. Brasil, 56, 15385-000, Ilha Solteira, SP, Brazil
[b] Universidade Federal de Goiás (UFG), Instituto de Química, Avenida Esperança, s/n, Campus Samambaia, Goiânia, GO, Brazil
[c] Universidade Estadual Paulista (Unesp), Instituto de Química. Av. Prof. Francisco Degni, 55 - Jardim Quitandinha, Araraquara, SP, 14800-900, Araraquara, Brazil
[d] Universidade Federal de São Carlos – UFSCar, LIEC. Rodovia Washington Luís, s/n, 13565-905, São Carlos, SP, Brazil
[e] Universidade Estadual Paulista (UNESP), Câmpus Experimental de Rosana, Brazil

ARTICLE INFO

Keywords:
A. Composites
C. Impedance spectroscopy
D. Dielectric properties
D. Acoustical properties

ABSTRACT

Cement/polyurethane based piezo composite was fabricated with 1-0–3 connectivity. Microstructural analysis shows that **polyurethane (PU)** acts as a binder, reducing the porosity and improving the matrix adhesion to the piezoelectric phase. Dielectric characterisation shows that PU strongly reduces both the interfacial polarisation process and the ionic mobility in the matrix, thus decreasing the dielectric constant and increasing the values of **voltage constant (g_{33})** and **electromechanical coupling coefficient (k_t)**. The composite was surface mounted on a **porous** concrete bar and evaluated as an **acoustic emission sensor (AE)**. The results show that this material is a highly sensitive sensor for AE detection in the frequency range 50–220 kHz.

1. Introduction

Recent advances in the development of sensors have made strong contributions in terms of the use of non-destructive evaluation (NDE) techniques, in fields such as aerospace structures and civil engineering [1–5]. The rate of construction of large buildings for housing or industry is increasing, and information about the performance of these buildings and data that can be used to predict their lifetimes are important, not only to prevent extensive damage and lower maintenance costs but primarily to prevent loss of life.

Since the structure of a building deteriorates over time, monitoring of structural integrity needs to be effective in terms of time and cost, and must be feasible [6–9]. Sensors are essential components in monitoring, and among of them piezoelectric sensors has appeared as one of the most efficient for acoustic emission technique [7,10,11]. Although PZT ceramic and polymer-based piezoelectric composites have been studied and proposed as AE sensors for **structural health monitoring (SHM)** [12,13], PZT ceramic and piezo polymers do not work well with concrete, which is the main material used in civil engineering. This is because of the differences in the dielectric constants and acoustic impedances of structural and sensor materials [14]. To try to overcome this problem, cement-based piezoelectric composites have been proposed with varying connectivities [5,15–25]. **Gong et al. [26–28], in an extensive work, has shown that inserting different conductive particles into 0–3 piezoelectric cement-based composites can promote not only an increase in the piezoelectric coefficient (d_{33}), but also the voltage factors (g_{33}). Qin [29], showed that 0–3 cement-based/PZT piezoelectric sensor has higher broad-band frequency response compared with the sensor made of PZT. Dong et al. [30], fabricated 2–2 cement based piezoelectric composites by using arranging-casting method, and demonstrated that they have properties of sensor and actuator with potential for application in civil engineering. Dongyu et al. [31], fabricated laminated 2-2 connectivity cement/polymer based piezoelectric composites with varied piezoelectric phase distribution, showing the influence of piezoelectric and matrix phases dimensions on g_{33} and dielectric loss (tg δ). Although advances have been made in the development of cement-based piezoelectric composites since the first publication performed by Li et al. [32]**, problems related to the acoustic scattering arising from the porosity of cement, and the mismatch in the dielectric constants and acoustic impedances of structural and sensor materials, still persist. Of the numerous piezoelectric cement-based composites that have been studied, we focus on the 1–3 connectivity composites. These consist of ceramic rods embedded in a cement matrix with a regular, ordered arrangement. Over the last few years, these composites have been widely studied, mainly

* Corresponding author.
E-mail address: alex.o.sanches@unesp.br (A.O. Sanches).

https://doi.org/10.1016/j.materresbull.2019.110541
Received 20 March 2019; Received in revised form 10 June 2019; Accepted 8 July 2019
Available online 09 July 2019
0025-5408/

in terms of their use as transducers and sensors, due to their low acoustic impedance (Z) and mechanical quality factor (Q_m) [5,16,18,20,22–24,26–29]. Contrary to the behaviour observed in 0–3 piezoelectric composites, the piezoelectric ceramic in 1–3 piezoelectric composites is exposed to the direct action of the electric field of polarisation. This causes strong polarisation of the ceramic, resulting in higher values of the piezoelectric coefficient (d_{33}) within shorter times and under smaller electric fields of polarisation. Depending on aspects such as the matrix, geometry, conditions of preparation and composition, 1–3 piezoelectric composites may have a high k_t, which, together with the high value of d_{33}, makes them excellent candidates for sensor devices [5,16,18,20,22–24,26–29]. The literature provides a wide range of techniques for the production of 1–3 connectivity composites, including ultrasonic cutting, injection moulding, lost moulding, laser machining, co-extrusion, lamination and fibre insertion methods [5,18,20,22,33–39], which are expensive to carry out [37–39]. The simplest techniques for producing 1–3 composites are the dice-fill and rod placement methods. However, problems related mainly to the conductivity of cement limit the polarisation of 1–3 composites directly prepared by the rod placement technique; this means that the main production technique for this type of composite is dice-fill, which requires on average 14 days to obtain a functional composite [5,16,18,20,22,24,25]. This paper reports a study of the use of a composite cement/polyurethane matrix for the manufacture of 1-0–3 connectivity composites, using PZT as piezoelectric phase, produced by the rod placement technique. We propose the idea that the dielectric and acoustic properties of the composite can be modified and adjusted by the presence of polymer in the sample, thus improving the dielectric and acoustic properties depending on the PU fraction, and reducing the electrical conductivity, allowing direct composite polarisation for earlier curing ages. A further aim of using this mixture is to bring the electromechanical properties of the sensor closer to those of the structure, for better electromechanical matching and to reduce the acoustic scattering by reducing the matrix porosity, contrary to the expected effect.

2. Methods

2.1. Materials

Nonionic aliphatic polyether-based PU was kindly supplied by Chemtura S.A. in a water dispersion form called PUW320. Lead zirconate titanate (PZT) powder was purchased from American Piezo Ceramics – APC, identified as PZT 851. Cement Portland CP II Z32 (Itaú) was utilised as the matrix and silver ink MhCondux MY203 from MHNano was utilised as the electrode.

2.2. Experimental

2.2.1. PZT wire

PZT wire was obtained from PZT powder mixed with PUW320 aqueous dispersion, using the relation below:

$$M_c = M_p \frac{\rho_c}{\rho_p}\left(\frac{\varnothing_c}{1-\varnothing_c}\right) \quad (1)$$

Where M is the mass, ρ is the density and ϕ_c is the mass fraction. The subscripts c and p refer to the ceramic and polymer phase, respectively. The density of PZT 851 was 7.6 g/cm^3 and that of PUW320 was 1.04 g/cm^3, according to the manufacturers. PZT powder was mixed with the PU solution (99/1 w/w) and the product was extruded in the form of wire onto a hot glass substrate and dried for 20 min in an oven at 70 °C (Fig. 1). After drying, the PZT wire was cut into the desired size and placed into an alumina container with an appropriate amount of lead oxide. Thermal treatment was applied at 350 °C over 4 h at a heating rate of 5 °C/min to remove organic matter. Following this, the temperature was increased to 1260 °C for 2 h to achieve sintering. The mean PZT rod diameter after sintering was 1.7 mm, with an aspect ratio of 0.97.

2.2.2. Composite preparation

PZT rod was placed in a square Teflon mould with dimensions 20 × 20 x 3.5 mm and filled with a mixture of cement paste (water/cement ratio = 0.5) and PU polymer in proportions of 10.5 and 21% w/w. The w/c ratio was maintained at a constant value for all the mixtures. The composites were cured for seven days, and were then polished on both surfaces to a thickness of around 1.0 mm. The surfaces of the sample were then cleaned with acetone and a thin layer of silver paint was coated on the surfaces to form electrodes (Fig. 1). The spacing of the ceramic rods was 1 mm, and the volume fraction of PZT was kept at 25%. For identification, the composites were designated CP (X%), where X indicates the weight fraction of PU.

2.3. Composite characterisation

The poling process of the composites was carried out using a Trek High Voltage Power Supply model 610, in a silicone oil bath at a controlled temperature. An electric field of E = 1.0 MV/m was applied for 30 min at 50 °C for polarisation. After poling, the longitudinal piezoelectric coefficient d_{33} was measured with a d_{33} piezo tester. Three samples were used in order to obtain mean values. The dielectric properties of the manufactured composite samples were measured using an SI 1260 Solartron impedance analyser with 1296 dielectric interface. The impedance characteristics of the composites were collected in the frequency range 10^0–10^6 Hz at room temperature. The voltage applied was 1 μV.

The dielectric constant ε_r and piezoelectric voltage factor g_{33} for each sample were calculated using the following equations:

$$\varepsilon_r = \frac{Cd}{\varepsilon_0 A} \quad (2)$$

$$g_{33} = \frac{d_{33}}{\varepsilon_0 \varepsilon_r} \quad (3)$$

where d and A are the thickness and electrode area of the sample, respectively; and ε_0 is the vacuum permittivity (8.85×10^{-12} F/m). The capacitance C was measured at 1 kHz. The thickness electromechanical coupling coefficient k_t was calculated from the plot of electric impedance versus frequency, using Eq. (4).

$$k_t^2 = \frac{\pi}{2}\frac{f_s}{f_p} tan\left(\frac{\pi}{2}\frac{f_p - f_s}{f_p}\right) \quad (4)$$

where f_s and f_p are the series and parallel resonance frequency, respectively, and can be approximated by

$$k_t^2 = \frac{\pi}{2}\frac{f_s}{f_p} tan\left(\frac{\pi}{2}\frac{f_n - f_m}{f_n}\right) \quad (5)$$

The electrical conductivity in the dc regime was obtained by the two-probe method using a voltage/current source (Keithley Instruments model 247, high voltage supply). A voltage was applied to the sample for 10 min and the current measurement was then performed. For acoustic emissions testing, the piezo sensor was surface-mounted on a porous cement block with dimensions of 190 × 90 x 50 mm. A pencil-lead break (also known as the Hsu-Nielsen method) conforming to ASTM standards was used as a simulated AE source. The detected signals were recorded directly using a digital storage oscilloscope Agilent model DS06012A with no amplification. The sensors were also tested using a ball-bearing drop as a simulated AE source, which produces high-amplitude and low-frequency stress waves. The ability of the sensors to detect AE at different distances from the source and with different energies was analysed.

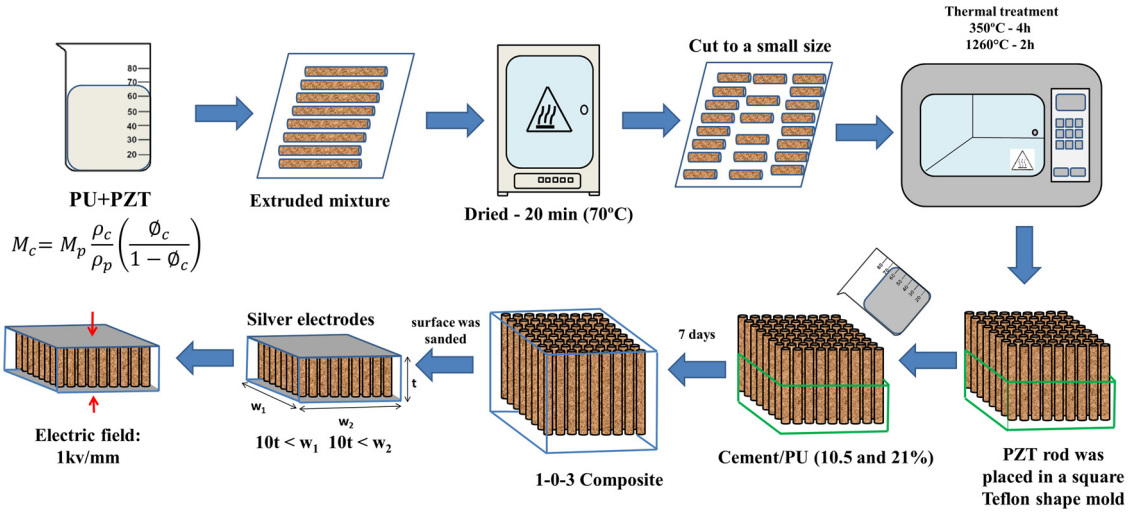

Fig. 1. Schematic diagram for fabrication of 1-0–3 type PZT/cement composite.

3. Results

Fig. 2 shows composite micrographs as a function of the polymer insertion, with an emphasis on the interface region between the ceramic rods and the matrix. It can be observed that the cement matrix has a porous structure with small fibrous crystals characteristic of the formation of hydrated calcium silicate (C-S-H **gel**). The low level of interaction between the matrix and the ceramic column can clearly be seen from the division and presence of spaces between the phases, as a result of the reduced adhesion between them. It can be observed that at lower concentrations of polymer, the matrix acquires the typical porous structure of the cement, and exhibits the formation of acicular crystals in large quantities corresponding to the presence of hydrated calcium trisulfoaluminate, also known as ettringite (C-A-S-H). In the same way, the low interaction between the matrix and the ceramic **rods** can be detected in the CP (10.5%) composites based on the division and presence of spaces between the phases (Fig. 2). In contrast, the CP (21%) composites have small pores, indicating a smoother matrix with higher adhesion to the surface of the ceramic rods, clearly due to the presence of PU.

Table 1 shows the values of the electrical conductivity for the CP (X %) composites and their individual phases. The electrical conductivity obtained for Cement Portland CP II Z32 after seven days of curing was $\sigma = 1.44 \times 10^{-7}$ S/cm. Conductivity values measured for later periods (14 days) showed a reduction of one or two orders of magnitude, which is in agreement with the values reported in the literature [26,40–46].

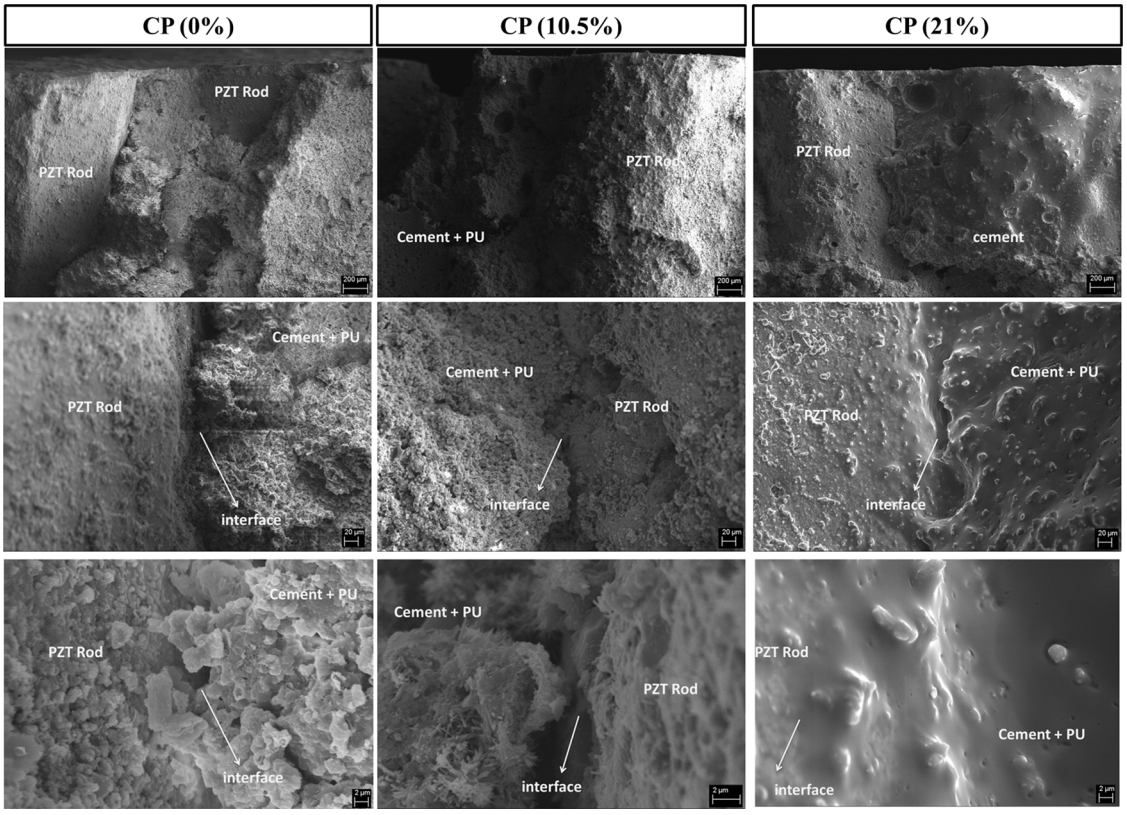

Fig. 2. Composite micrographs at the interface region between the ceramic columns as a function of PU content.

Table 1
Values of ε_r, g_{33} and d_{33} for cement, PU and 1–3 and 1-0–3 composites.

Sample	ε_r (1 kHz)	g_{33} (mV.m/N)	d_{33} (pC/N)	**tg δ (1 kHz)**	σ (S/cm)
PZT	1950	25	400	**0.015**	9.25×10^{-11}
Cement	69	–	–	**0.8**	1.44×10^{-7}
PU	6	–	–	**0.04**	1.98×10^{-12}
CP (0%)	282	–	–	**0.22**	1.52×10^{-8}
CP (10.5%)	424	67	251	**0.14**	1.07×10^{-10}
CP (21%)	225	127	253	**0.12**	3.75×10^{-11}

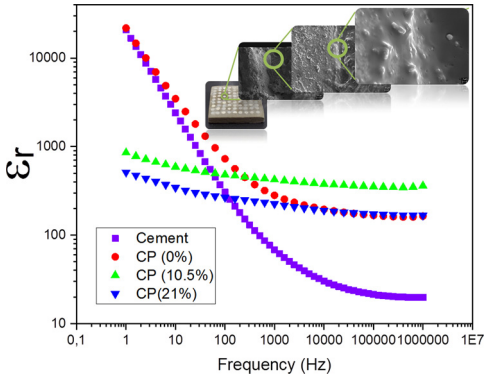

Fig. 3. Relative permittivity of the cement, 1–3 and 1-0–3 composites as a function of frequency. Inset: CP (21%) sample photo and SEM micrographs highlighting the PZT/matrix interface.

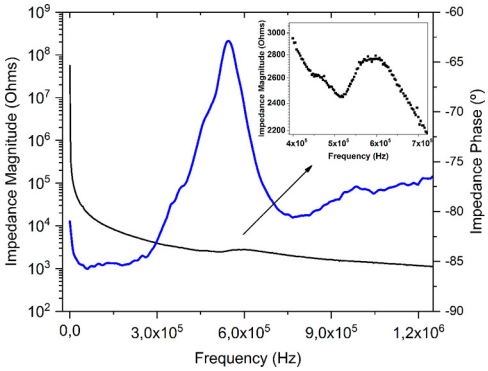

Fig. 4. Impedance and phase of CP (10.5%) as a function of frequency.

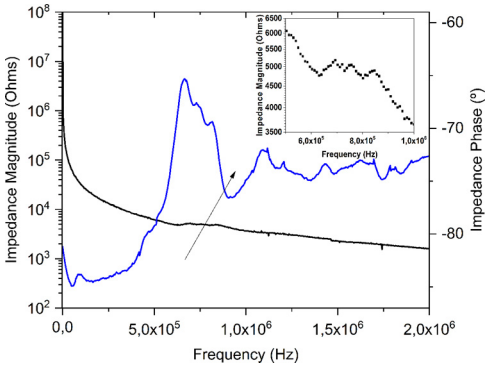

Fig. 5. Impedance and phase of CP (21%) as a function of frequency.

The electrical conductivity of the cement is related to the ionic concentration in the liquid phase, pore density, and also to its structural change. The CP (0%) sample had a value of $\sigma = 1.52 \times 10^{-8}$ S/cm, one order of magnitude lower than the cement matrix. This difference in conductivity can be attributed to the type of connectivity system

Table 2
Electroacoustic characteristics of cement, PZT and PZT/PU/cement composite.

	Cement	PZT	**CP (0%)**	CP (10.5%)	CP (21%)
ρ x 10^3 (kg. m^{-3})	3.15	7.6	**4.90**	3.20	3.09
N_t ($m.s^{-1}$)	1587	2040	**2074**	1704	1513
Z x 10^6 (kg. $m^{-2}.s^{-1}$)	~10	~31	**10**	10	9.38
k_t (%)	–	51	–	64.63	69.26
Q_m	–	80	–	5.13	5.23

making polarisation of the **CP (0%)** sample impossible. However, the addition of up to 21% w/w of PU to the composites allowed the proportion of PU in the composite to interrupt the conduction path of the ionic charges, decreasing its conductivity and allowing the samples to be polarised after seven days of curing.

The average values of the longitudinal piezoelectric constant d_{33}, the dielectric constant at 1 kHz and the voltage piezoelectric constant g_{33} are also shown in Table 1. It can be observed that both composite samples have almost the same values of d_{33}, indicating a saturation threshold for polarisation.

The dielectric constant behaviour of the cement and composites with different PU weight fractions as a function of frequency is shown in Fig. 3. High values of ε_r, reaching values of up to 10^4, can be observed for cement for frequencies lower than 1 kHz. These values of the dielectric constant for pure cement cannot be attributed solely to interfacial polarisation phenomena arising from the microstructures of the cement and from the ionic movement into the porous or electrode polarisation. Coverdale et al. [47] observed a similar result, attributing it to the existence of amplification mechanisms originating from the existence of conducting channels (capillary pores) that extend throughout the geometry of the sample, obstructed only by thin insulating barriers. Thus, each channel contributes an extremely high capacitance in terms of the dielectric sample response, and this tends to decrease with curing time and the formation of hydration products. When the frequency is increased, the dielectric constant decreases due to the lower contributions of interfacial and ionic polarisation, or even electrode polarisation. In CP (0%), the high conductivity term of the cement phase contributes significantly at lower frequencies. For the 1-0–3 composites, the dielectric constant showed a lower variation as a function of frequency compared to cement and the CP (0%) sample. **In addition, was verified a loss tangent (tan δ) reduction by adding PU in the composite (**Table 1**).These behaviours were** attributed to the PU fraction in the matrix, which reduces both the porosity and the amplification mechanisms based on capillary systems. PU acts as a binder, strongly reducing both the interfacial polarisation process and the ionic mobility in the matrix. An increase of g_{33} occurs with a reduction in the dielectric constant (Table 1), meaning that the sensitivity to the received voltage increases, which is a desirable characteristic for a piezoelectric sensor. It is important to note the influence of PU on the composites with increasing PU content. In a frequency range of above 1 kHz, the relative permittivity of the composite becomes closer to the relative permittivity of the pure cement, the main structural material used in civil engineering. A dielectric constant of the sensor that is close to that of the material to which it is attached is very important, since this generates less distortion and reduction of the received signal.

Figs. 4 and 5 show the impedance and phase spectra of the CP (10.5%) and CP (21%) composites. In both composites, the impedance initially decreases sharply and then changes smoothly with an increase in the frequency. Moreover, the shape of resonant peak becomes more irregular as the PU content increases, as shown in the inset to Figs. 5 and 6. The electromechanical coupling coefficients k_t was determined from the resonance peak using Eq. (4), and the results are shown in Table 2. It was found that the k_t value of the composites was higher than for pure PZT, and this was attributed to the design of the composite [48]. The ability of the matrix to allow deformations along the thickness of the ceramic allied to the own composite surface

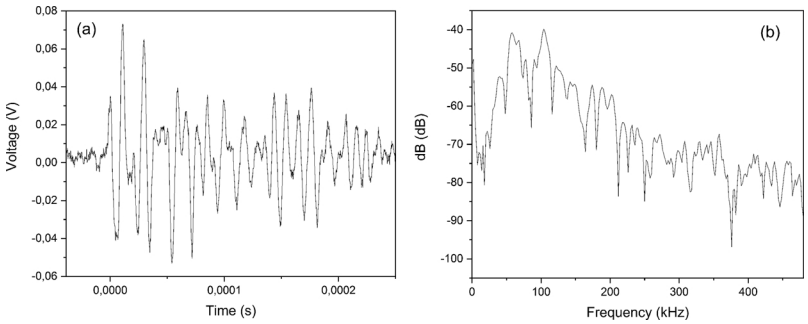

Fig. 6. a) Sensor response to a pencil-lead break in the time domain; b) fast Fourier. Transform.

Table 3
Comparative electroacoustic properties of 1–3 composites.

	Vol. (%)	ε_r (1 kHz)	g_{33} (mV.m/N)	d_{33} (pC/N)	Z x 10^6 (kg. $m^{-2}.s^{-1}$)	k_t (%)	Reference
BNT	30%	~170	~ 67	~ 45	~8	~16	[24]
$BaZr_{0.05}Ti_{0.95}O_3$	40%	450	20	79	~9	–	[25]
$BaTiO_3$	30%	300	23	~ 60	–	–	[18]
PMN	22.7%	277.79	–	250	10	53.26	[16]
PZT8	25%	–	–	~115	~10.5	~55	[51]
CP (21%)	25%	225	127	253	9.38	69.26	**this work**

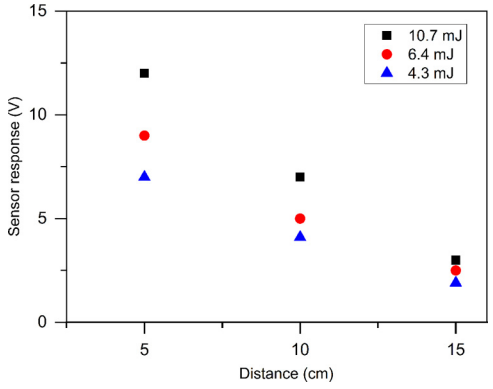

Fig. 7. Sensor response to ball-bearing drop AE source.

deformation caused by the displacement of the ceramic columns gives the 1–3 composites high values of k_t of between 0.6 and 0.7 [36,48–50]. With presence and an increase in the PU content, the matrix becomes softer and the movement of the PZT **rods** is facilitated, resulting in a rise in the electromechanical coupling factor k_t for the 1-0–3 composite. However, this fact means that other modes of coupled vibration may intensify in the composite with increasing PU content, as shown in Fig. 6.

The values of acoustic impedance are quite different for ceramic and cement, and this causes a high energy loss between the structure and the sensor in the interface region, reducing the monitoring performance of the PZT as an AE sensor. The acoustic impedance can be calculated from the equations

$$Z = \rho C_c = 2\rho N_t \quad (6)$$

$$N_t = f_s t$$

where C_c is the longitudinal wave velocity in the composite; ρ is the composite density; N_t is the constant of frequency; f_s is the frequency of minimal impedance; and t is the thickness of the composite sample.

The low value of N_t for cement compared to PZT was attributed to strong wave attenuation as a consequence of the waves being scattered by the porous and irregular microstructure of cement. Since the elastic modulus of the polymer is lower than that of the cement, we would expect an attenuation of acoustic waves in the cement as the incorporated polymer causes a lower energy transference to the ceramic [33]. However, high values of N_t were observed for the CP (10.5%) composite compared to cement. This was attributed to the effectiveness of the porosity reduction produced by PU, which acts as a binder at this proportion. A PU fraction of above 10.5% promoted greater longitudinal wave scattering in the composite, reducing the N_t values and directly reducing the acoustic impedance of the composites. However, even for a PU fraction of 21.0%, the acoustic impedance of the composite sample is close to that of the cement matrix, giving a high sensitivity of the sensor due to the low acoustic wave scattering in the composite/structure interface as a result of better impedance matching.

Table 3 shows the values of some electroacoustic properties of cementitious 1–3 composites found in the literature, as compared to the CP (21%). **In our work the k_t values is higher of those found in the literature for 1–3 composites, showing the effectiveness of the PU addition.**

For use in AE sensors monitoring structures in civil engineering, the piezoelectric composite must have a broadband frequency response and low mechanical quality, and its acoustic impedance and dielectric constant should match the acoustic impedance of the structural material. Fig. 6a shows the response of the 1-0–3 sensor CP (21%) in the time domain for a pencil-lead break (the Hsu-Nielsen method). A fast Fourier transform (FFT) was applied to obtain the response in the frequency domain, as shown in Fig. 6b. It can be seen that in the frequency range 50 kHz–220 kHz, the signal does not drop off and is relatively flat; this is a good characteristic for an AE sensor.

Fig. 7 shows the behaviour of the sensor in response to impact energy. A steel ball of mass 21.4 g was dropped onto the **porous** cement block, with varying energies and distances from the sensor. At 15 cm away from the AE source, the sensor response was around 2.0 V for a lower energy used (4.3 mJ). The noise level can be assumed to be around 2.0 mV, and it can therefore be concluded that the sensor is able to detect the stress wave occurring in the block. The sensor response is inversely proportional to distance, and it can therefore be shown by extrapolation that the sensor can detect an AE signal at a distance of around 18.5 cm away from the source, even for only 4.3 mJ. The maximum detection distance is limited by the porous structure of the cement block on which the sensor is located.

4. Conclusions

Cement-based piezoelectric composites were fabricated with 1–3 and 1-0–3 connectivity using a rod placement technique. The introduction of the PU into the cementitious matrix allowed the polarisation of the composite within the initial period of cure (seven days), giving a value for the piezoelectric coefficient d_{33} of 253 pC/N. The reduced porosity allowed stronger adhesion of the matrix to the ceramic column, making the matrix softer and increasing the k_t factor above the value for PZT. The addition of PU also changed the dielectric constant and consequently the g_{33} values, bringing the properties of the composite material closer to those of the structural material (cement block). In addition, the characteristics of the composite, such as mechanical quality factors, acoustic impedance and dielectric constant, become better than that of the PZT ceramic for the detection of acoustic emissions.

Acknowledgements

The authors express their gratitude to Fundação de Amparo à Pesquisa do Estado de São Paulo – FAPESP (CEPID – CDMF Grant 2013/07296-2), Coordenação de Aperfeiçoamento de Pessoal de Nível Superior (CAPES) and Conselho Nacional de Desenvolvimento Científico e Tecnológico (CNPq) for the financial support and scholarship.

References

[1] H.S. Yoon, D. Jung, J.H. Kim, Lamb wave generation and detection using piezoceramic stack transducers for structural health monitoring applications, Smart Mater. Struct. 21 (2012), https://doi.org/10.1088/0964-1726/21/5/055019.
[2] H. Ning, T. Shimomukai, H. Fukunaga, S. Zhongqing, Damage identification of metallic structures using A0 mode of lamb waves, Struct. Heal. Monit. 7 (2008) 271–285, https://doi.org/10.1177/1475921708090566.
[3] V. Giurgiutiu, A. Zagrai, J.J. Bao, Piezoelectric wafer embedded active sensors for aging aircraft structural health monitoring, Struct. Heal. Monit. 1 (2002) 41–61, https://doi.org/10.1177/147592170200100104.
[4] E. Dehghan Niri, S. Salamone, A probabilistic framework for acoustic emission source localization in plate-like structures, Smart Mater. Struct. 21 (2012), https://doi.org/10.1088/0964-1726/21/3/035009.
[5] L. Qin, S. Huang, X. Cheng, Y. Lu, Z. Li, The application of 1-3 cement-based piezoelectric transducers in active and passive health monitoring for concrete structures, Smart Mater. Struct. 18 (2009), https://doi.org/10.1088/0964-1726/18/9/095018.
[6] Y. Yang, Y. Hu, Y. Lu, Sensitivity of PZT Impedance Sensors for Damage Detection of Concrete Structures, Sensors 8 (2008) 327–346, https://doi.org/10.3390/s8010327.
[7] B. Shen, X. Yang, Z. Li, A cement-based piezoelectric sensor for civil engineering structure, Mater. Struct. Constr. 39 (2006) 37–42, https://doi.org/10.1617/s11527-005-9021-8.
[8] C.U. Grosse, M. Krüger, C. Materials, Wireless acoustic emission sensor networks for structural health monitoring in civil engineering, Techniques (2006) 1–8.
[9] A. Nair, C.S. Cai, Acoustic emission monitoring of bridges: review and case studies, Eng. Struct. 32 (2010) 1704–1714, https://doi.org/10.1016/j.engstruct.2010.02.020.
[10] S. Barré, M.L. Benzeggagh, On the use of acoustic emission to investigate damage mechanisms in glass-fibre-reinforced polypropylene, Compos. Sci. Technol. 52 (1994) 369–376, https://doi.org/10.1016/0266-3538(94)90171-6.
[11] N. Saber, Q. Meng, H.Y. Hsu, S.H. Lee, H.C. Kuan, D. Marney, N. Kawashima, J. Ma, Smart thin-film piezoelectric composite sensors based on high lead zirconate titanate content, Struct. Heal. Monit. 14 (2015) 214–227, https://doi.org/10.1177/1475921714560075.
[12] M.P. Wenger, P. Blanas, R.J. Shuford, D.K. Das-Gupta, Characterization and evaluation of piezoelectric composite bimorphs for in-situ acoustic emission sensors, Polym. Eng. Sci. 39 (1999) 508–518, https://doi.org/10.1002/pen.11441.
[13] M. Rguiti, S. Grondel, F. El Youbi, C. Courtois, M. Lippert, A. Leriche, Optimized piezoelectric sensor for a specific application: detection of Lamb waves, Sensors Actuators, A Phys. 126 (2006) 362–368, https://doi.org/10.1016/j.sna.2005.10.015.
[14] R. Rianyoi, R. Potong, N. Jaitanong, R. Yimnirun, A. Chaipanich, Dielectric, ferroelectric and piezoelectric properties of 0-3 barium titanate-Portland cement composites, Appl. Phys. A Mater. Sci. Process. 104 (2011) 661–666, https://doi.org/10.1007/s00339-011-6307-2.
[15] P. Chomyen, R. Potong, R. Rianyoi, A. Ngamjarurojana, P. Chindaprasirt, A. Chaipanich, Microstructure, dielectric and piezoelectric properties of 0–3 lead free barium zirconate titanate ceramic-Portland fly ash cement composites, Ceram. Int. 44 (2018) 76–82, https://doi.org/10.1016/j.ceramint.2017.09.112.
[16] Z. Li, S. Huang, L. Qin, X. Cheng, An Investigation on 1–3 Cement Based Piezoelectric Composites, (2007), https://doi.org/10.1088/0964-1726/16/4/007.
[17] X. Dongyu, C. Xin, S. Banerjee, W. Lei, Dielectric, Piezoelectric and Damping Properties of Novel 2-2 Piezoelectric Composites, (2015), https://doi.org/10.1088/0964-1726/24/2/025003.
[18] R. Rianyoi, R. Potong, A. Ngamjarurojana, R. Yimnirun, R. Guo, A.S. Bhalla, A. Chaipanich, Acoustic, dielectric and piezoelectric properties of 1-3 connectivity barium titanate-portland cement composites, Ferroelectrics 452 (2013) 76–83, https://doi.org/10.1080/00150193.2013.841519.
[19] H. Zhou, Y. Liu, Y. Lu, P. Dong, B. Guo, W. Ding, F. Xing, T. Liu, B. Dong, In-situ crack propagation monitoring in mortar embedded with cement-based piezoelectric ceramic sensors, Constr. Build. Mater. 126 (2016) 361–368, https://doi.org/10.1016/j.conbuildmat.2016.09.050.
[20] S.H. Zhai, Y.C. Wang, B. Geng, H.C. Xu, S.F. Huang, Study on the 1-3 orthotropic polymer/cement based piezoelectric composite, Proc.2016 Symp. Piezoelectricity, Acoust. Waves Device Appl. SPAWDA 2016 (2017) 37–40, https://doi.org/10.1109/SPAWDA.2016.7829951.
[21] S.F. Huang, M.M. Li, D.Y. Xu, M.J. Zhou, S.H. Xie, X. Cheng, Investigation on a kind of embedded AE sensor for concrete health monitoring, Res. Nondestruct. Eval. 24 (2013) 202–210, https://doi.org/10.1080/09349847.2013.789949.
[22] R. Potong, R. Rianyoi, A. Ngamjarurojana, A. Chaipanich, Microstructure and performance of 1–3 connectivity environmental friendly lead-free BNBK-Portland cement composites, Mater. Res. Bull. 90 (2017) 59–65, https://doi.org/10.1016/j.materresbull.2017.02.008.
[23] R.E. Newnham, D.P. Skinner, L.E. Cross, Connectivity and piezoelectric-pyroelectric composites, Mater. Res. Bull. 13 (1978) 525–536, https://doi.org/10.1016/0025-5408(78)90161-7.
[24] R. Rianyoi, R. Potong, A. Ngamjarurojana, Acoustic and electrical properties of 1–3 connectivity bismuth sodium titanate – portland cement composites, Mater. Res. Bull. 60 (2014) 353–358, https://doi.org/10.1016/j.materresbull.2014.08.049.
[25] R. Potong, R. Rianyoi, A. Ngamjarurojana, A. Chaipanich, Dielectric and piezoelectric properties of 1–3 non-lead barium zirconate titanate-Portland cement composites, Ceram. Int. 39 (2013) S53–S57, https://doi.org/10.1016/j.ceramint.2012.10.034.
[26] H. Gong, Y. Zhang, J. Quan, S. Che, Preparation and properties of cement based piezoelectric composites modified by CNTs, Curr. Appl. Phys. 11 (2011) 653–656, https://doi.org/10.1016/j.cap.2010.10.021.
[27] H. Gong, Z. Li, Y. Zhang, R. Fan, Piezoelectric and dielectric behavior of 0-3 cement-based composites mixed with carbon black, J. Eur. Ceram. Soc. 29 (2009) 2013–2019, https://doi.org/10.1016/j.jeurceramsoc.2008.11.014.
[28] H. Gong, Y. Zhang, S. Che, Influence of carbon black on properties of PZT-cement piezoelectric composites, J. Compos. Mater. 44 (2010) 2747–2757, https://doi.org/10.1177/0021998310371550.
[29] L. Qin, Y. Lu, Z. Li, Embedded cement-based piezoelectric sensors for acoustic emission detection in concrete, J. Mater. Civ. Eng. 22 (2010) 1323–1327, https://doi.org/10.1061/(ASCE)MT.1943-5533.0000133.
[30] B. Dong, Z. Li, Cement-based piezoelectric ceramic smart composites, Compos. Sci. Technol. 65 (2005) 1363–1371, https://doi.org/10.1016/j.compscitech.2004.12.006.
[31] X. Dongyu, C. Xin, S. Banerjee, H. Shifeng, Design, fabrication, and properties of 2-2 connectivity cement/polymer based piezoelectric composites with varied piezoelectric phase distribution, J. Appl. Phys. 116 (2014) 0–7, https://doi.org/10.1063/1.4904931.
[32] Z. Li, D. Zhang, K. Wu, Cement-based 0-3 piezoelectric composites, J. Am. Ceram. Soc. 85 (2002) 305–313.
[33] B. Geng, D. Xu, S. Yi, G. Gao, H. Xu, X. Cheng, Design and properties 1–3 multi-element piezoelectric composite with low crosstalk effects, Ceram. Int. 43 (2017) 15167–15172, https://doi.org/10.1016/j.ceramint.2017.08.047.
[34] S.F. Huang, X.J. Lin, D.Y. Xu, M.J. Zhou, M.M. Li, S.H. Xie, X. Cheng, Preparation and performance of 1-3 multi-element piezoelectric composites, Ceram. Int. 41 (2015) 6759–6763, https://doi.org/10.1016/j.ceramint.2015.01.122.
[35] X. Dongyu, C. Xin, G. Hongda, L. Fan, H. Shifeng, Design, fabrication and properties of 1-3 piezoelectric ceramic composites with varied piezoelectric phase distribution, Ceram. Int. 41 (2015) 9433–9442, https://doi.org/10.1016/j.ceramint.2015.03.324.
[36] M.S. Mirza, Q. Liu, T. Yasin, X. Qi, J.F. Li, M. Ikram, Dice-and-fill processing and characterization of microscale and high-aspect-ratio (K, Na)NbO3-based 1-3 lead-free piezoelectric composites, Ceram. Int. 42 (2016) 10745–10750, https://doi.org/10.1016/j.ceramint.2016.03.198.
[37] H.J. Lee, S. Zhang, Y. Bar-Cohen, S. Sherrit, High temperature, high power piezoelectric composite transducers, Sensors (Switzerland) 14 (2014) 14526–14552, https://doi.org/10.3390/s140814526.
[38] R. Rouffaud, F. Levassort, M.P. Thi, C. Bantignies, M. Lethiecq, A.C. Hladky-Hennion, Super-cell piezoelectric composite with 1-3 connectivity, IEEE Trans. Ultrason. Ferroelectr. Freq. Control 63 (2016) 2215–2223, https://doi.org/10.1109/TUFFC.2016.2606109.
[39] K.S. Ramadan, D. Sameoto, S. Evoy, A review of piezoelectric polymers as functional materials for electromechanical transducers, Smart Mater. Struct. 23 (2014), https://doi.org/10.1088/0964-1726/23/3/033001.
[40] X. Wei, Z. Li, Early hydration process of portland cement paste by electrical measurement, J. Mater. Civ. Eng. 18 (2006) 99–105, https://doi.org/10.1061/(ASCE)0899-1561(2006)18:1(99).
[41] M.S. Morsy, Effect of temperature on electrical conductivity of blended cement pastes11This paper was originally submitted to advanced cement based materials, The Paper Was Received at the Editorial Office of Cement and Concrete Research on 27 August 1998 and Accepte, Cem. Concr. Res. 29 (1999) 603–606, https://doi.org/

10.1016/S0008-8846(98)00198-7.
[42] D.D.L. Chung, Electrical conduction behavior of cement-matrix composites, J. Mater. Eng. Perform. 11 (2002) 194–204, https://doi.org/10.1361/105994902770344268.
[43] K.A. Snyder, X. Feng, B.D. Keen, T.O. Mason, Estimating the electrical conductivity of cement paste pore solutions from OH-, K + and Na + concentrations, Cem. Concr. Res. 33 (2003) 793–798, https://doi.org/10.1016/S0008-8846(02)01068-2.
[44] M.R. Nokken, Electrical conductivity to determine maturity and activation energy in concretes, Mater. Struct. Constr. 49 (2016) 2209–2221, https://doi.org/10.1617/s11527-015-0644-0.
[45] F. Rajabipour, J. Weiss, Electrical conductivity of drying cement paste, Mater. Struct. Constr. 40 (2007) 1143–1160, https://doi.org/10.1617/s11527-006-9211-z.
[46] K.R. Backe, O.B. Lile, S.K. Lyomov, Characterizing curing cement slurries by electrical conductivity, SPE Drill. Complet. 16 (2001), https://doi.org/10.2118/74694-PA 207–207.
[47] R.T. Coverdale, B.J. Christensen, T.O. Mason, H.M. Jennings, E.J. Garboczi, Interpretation of the impedance spectroscopy of cement paste via computer modelling - Part II Dielectric response, J. Mater. Sci. 29 (1994) 4984–4992, https://doi.org/10.1007/BF01151088.
[48] Ralf Steinhausen, Modelling and characterization of piezoelectric 1-3 fibre composites, Sens. Proc. (2011) 199–204, https://doi.org/10.5162/sensor11/a8.4.
[49] H. Taunaumang, I.L. Guy, H.L.W. Chan, Electromechanical properties of 1-3 piezoelectric ceramic/piezoelectric polymer composites, J. Appl. Phys. 76 (1994) 484–489, https://doi.org/10.1063/1.357099.
[50] M.S. Mirza, T. Yasin, M. Ikram, M.N. Khan, M. Shuaib, Fabrication of 1–3 connectivity (Ba0.95Pb0.05)(Ti0.99Co0.01)O3/monothane-A70 composites by die-pressing method and their electrical characterizations, Ceram. Int. 40 (2014) 11477–11484, https://doi.org/10.1016/j.ceramint.2014.03.155.
[51] K.H. Lam, H.L.W. Chan, Piezoelectric cement-based 1-3 composites, Appl. Phys. A Mater. Sci. Process. 81 (2005) 1451–1454, https://doi.org/10.1007/s00339-005-3226-0.